Detecting dependencies between spike trains of pairs of neurons through copulas

Sacerdote, Laura ; Tamborrino, Massimiliano; Zucca, Cristina

Published in:
Brain Research

DOI:
10.1016/j.brainres.2011.08.064

Publication date:
2011

Document version
Publisher's PDF, also known as Version of record

Citation for published version (APA):
Sacerdote, L., Tamborrino, M., & Zucca, C. (2011). Detecting dependencies between spike trains of pairs of neurons through copulas. *Brain Research*, *1434*, 243-256. https://doi.org/10.1016/j.brainres.2011.08.064

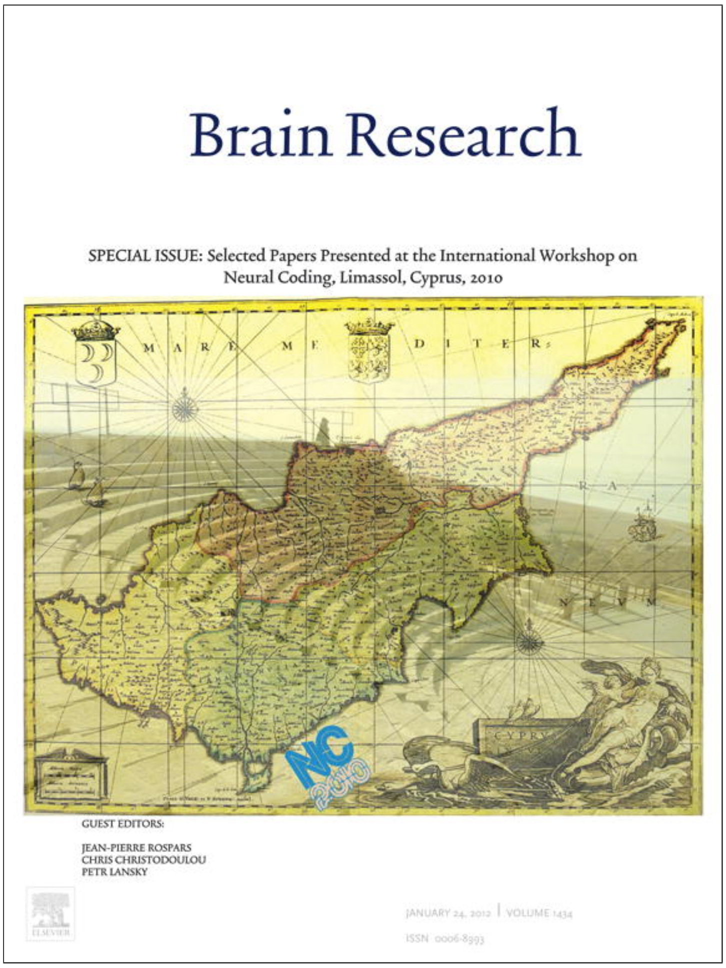
Brain Research
SPECIAL ISSUE: Selected Papers Presented at the International Workshop on Neural Coding, Limassol, Cyprus, 2010
GUEST EDITORS:
JEAN-PIERRE ROSPARS
CHRIS CHRISTODOULOU
PETR LANSKY
JANUARY 24, 2012 | VOLUME 1434
ISSN 0006-8993

BRAIN RESEARCH 1434 (2012) 243–256

Available online at www.sciencedirect.com

SciVerse ScienceDirect

www.elsevier.com/locate/brainres

ELSEVIER

BRAIN RESEARCH

Research Report

Detecting dependencies between spike trains of pairs of neurons through copulas

Laura Sacerdote[a,b], *Massimiliano Tamborrino*[c,*], *Cristina Zucca*[a,b]

[a]*Department of Mathematics "G. Peano", University of Turin, Via Carlo Alberto 10, Turin, Italy*
[b]*Neuroscience Institute of Turin (NIT), University of Turin, Regione Gonzole 10, Orbassano (Turin), Italy*
[c]*Department of Mathematical Sciences, University of Copenhagen, Universitetsparken 5, Copenhagen, Denmark*

ARTICLE INFO

Article history:
Accepted 29 August 2011
Available online 12 September 2011

Keywords:
Neural connectivity
Spike times
Leaky integrate and fire models
Diffusion processes
Copulas
Dependencies

ABSTRACT

The dynamics of a neuron are influenced by the connections with the network where it lies. Recorded spike trains exhibit patterns due to the interactions between neurons. However, the structure of the network is not known. A challenging task is to investigate it from the analysis of simultaneously recorded spike trains. We develop a non-parametric method based on copulas, that we apply to simulated data according to different bivariate Leaky Integrate and Fire models. The method discerns dependencies determined by the surrounding network, from those determined by direct interactions between the two neurons. Furthermore, the method recognizes the presence of delays in the spike propagation.
This article is part of a Special Issue entitled "Neural Coding".

1. Introduction

The knowledge of the structure of a network is helpful to understand principles of its organization. Unfortunately, the connections between neurons belonging to a specific or different areas of the brain are generally unknown. Experimental techniques will not allow to get such information in an immediate future. However, the analysis of recorded spike trains may suggest possible connections and help neuroscientists to reconstruct the structure of networks.

Raster displays might reveal the presence of dependencies between the interspike intervals (ISIs) of the observed neurons, reflecting the existence of connections in the network. To study its structure, one should first establish the dependencies between the recorded neurons, and then investigate the nature and the strength of these dependencies.

Since the pioneering work of Perkel et al. (1967), large efforts have been devoted to analyze simultaneously recorded data coming from several neurons. In the last thirty years, different techniques have been proposed; limits and difficulties are known, allowing their use in laboratories. There exists a lot of fundamental work on this subject. An exhaustive list of references can be found in a recent book (Grün and Rotter, 2010), where the available methods are collected, explained and discussed.

The most used methods to detect connections between neurons are based on the study of the crosscorrelation function (Perkel et al., 1967). Unfortunately, crosscorrelation de-

* *Corresponding author*. Fax: +45 35320704.
E-mail addresses: laura.sacerdote@unito.it (L. Sacerdote), mt@math.ku.dk (M. Tamborrino), cristina.zucca@unito.it (C. Zucca).

0006-8993/$ – see front matter © 2011 Elsevier B.V. All rights reserved.
doi:10.1016/j.brainres.2011.08.064

scribes linear dependencies and it might fail to detect nonlinearities (Sacerdote and Tamborrino, 2010).

Other techniques include Generalized Linear Models (GLMs) (Brillinger, 1988) with their variants (Stevenson et al., 2009). However, these methods present difficulties too. A typical problem is the dependence of the results upon the size of the testing window (Eldawlatly et al., 2009).

Updating an older paper (Borisyuk et al., 1985), Masud and Borisyuk (2011) propose to use the Cox method as a statistical method to analyze functional connectivity of simultaneously recorded multiple spike trains. It is based on the theory of modulated renewal processes (Cox, 1972). This method detects bivariate dependencies between multiple spike trains in a neural network, providing statistical estimates of the strengths of influence and their confidence intervals. Moreover, it presents a set of advantages with respect to the others, e.g. it does not depend on the window amplitude, it detects weak dependencies and it succeeds in the presence of spurious connection due to common source or indirect connections. However, it requests a preliminary estimation of a set of parameters that is a very difficult task if the underlying model is unknown. Therefore, the results may become unreliable.

We propose the use of the copula notion to detect possible dependencies between ISIs. Copulas are joint probability distributions with uniform marginal distributions (Nelsen, 2006). Therefore, they catch dependencies between random variables (rvs), and they can be easily used for modeling purposes, being scale-free.

In neuroscience, the use of copulas is not a novelty. Jenison and Reale (2004) show how to couple probability densities to get flexibility in the construction of a multivariate neural population. Furthermore, they express the mutual information between two ISIs in terms of the copula distribution. More recently, Onken et al. (2009) inferred the connectivity between neurons by fitting the spike counts through the copulas of a given family. In particular, they provide a method to estimate the parameters of the prescribed copula. Sacerdote and Sirovich (2010) propose to use copulas to model the coupling of two or more neurons, while Sacerdote and Tamborrino (2010) investigate the reliability of crosscorrelograms analysis to detect dependencies in spike trains with known connections, being simulated through copula models.

A spike train is a collection of spike times and it can be considered as a vector of rvs. Therefore, a copula between two spike trains can be determined. Different types of dependency correspond to different shapes of the copula.

The aim of this work is to illustrate the ability of copulas to recognize dependencies between spike trains coming from different underlying models. To do this, we propose a nonparametric method.

A detailed study on simulated data could allow to classify shapes of copulas corresponding to different kinds of connections. However, in this paper, our main goal is to detect dependencies, instead of classifying their nature. Indeed, it represents a long task, since it corresponds to determine the joint distribution, i.e. the copula, that fits the data.

Furthermore, we limit ourselves to the study of two spike trains. The extension to multiple dependencies arising in the case of a larger number of spike trains requests further mathematical effort. Indeed, in a network of n neurons, it would correspond to investigate dependencies in groups of k neurons, $k=2,\ldots,n$, i.e. to investigate k dimensional copulas for groups of k spike trains. However, our method can be applied immediately to the case of n spike trains, if the interest is focused on pairwise dependencies, as it happens in Masud and Borisyuk (2011). To do this, it is enough to select a target and a reference neuron, and then consider all the possible combinations.

In Section 2, we describe our method to catch dependencies between spike trains through copulas. In Section 3, we introduce the different Leaky Integrate and Fire (LIF) models used to generate coupled spike trains. In Section 4, we test the proposed method on those data. In Section 5, we discuss the results of our approach, providing a comparison with other methods, in particular with the Cox method. Finally, in Section 6, we describe conclusions, open problems and possible developments.

2. The copula method

2.1. *A mathematical tool: copulas*

A copula is a mathematical object that catches dependencies between rvs. In (Nelsen, 2006), it is defined as

Definition 1. A two-dimensional copula is a function C: $[0,1]^2 \to [0,1]$ with the following properties:

$$C(u;0) = C(0;v) = 0 \text{ and } C(u;1) = u; C(1;v) = v \text{ for every } u, v \in [0;1]; \tag{1}$$

$$C \text{ is } 2\text{–increasing, i.e. for every } u_1, u_2, v_1, v_2 \in [0;1] \text{ such that } u_1 \le u_2, v_1 \le v_2, \tag{2}$$

$$C(u_1, v_1) + C(u_2, v_2) - C(u_1, v_2) - C(u_2, v_1) \ge 0.$$

Let X and Y be two rvs with marginal cumulative distribution functions (cdfs) F and G, respectively. Let H (x, y) be the joint cdf of (X,Y). Due to the Sklar's theorem, a two dimensional copula C satisfies:

$$H(x, y) = C(F(x), G(y)) \; x, y \in \mathbb{R}. \tag{1}$$

This theorem holds also in the multivariate case (Nelsen, 2006).

From Eq. (1), it follows that a copula is a joint cdf with two standard uniform marginals. Therefore, copulas are scale-free and capture all the information related to the joint behavior, and do not involve the marginal distributions. Hence, the study of a bivariate distribution can be split in two parts: the marginal behaviors caught by the marginal cdfs and the dependencies contained in the copula structure.

Copulas have other properties, as for instance the invariance under strictly increasing transformations, or the possibility to model several joint distribution functions.

In the literature, there exists a list of families of copulas, e.g. the Archimedean and the Euclidean families. Given a sample, we may perform a goodness-of-fit test to test if the data could belong to a certain family (Genest et al., 2009).

After that, we may estimate the involved parameters as done by Genest and Favre (2007) or Onken et al. (2009).

To measure the strength of dependencies, we consider the Kendall's tau τ. It is a rank correlation index assuming values in [−1,1] and it measures the concordance for bivariate random vectors.

Given a data sample of size n, an estimator $\hat{\tau}$ of the Kendall's tau is given by:

$$\hat{\tau} = \frac{n_c - n_d}{\frac{1}{2}n(n-1)},$$

Here, n_c and n_d denote the number of concordant and discordant pairs in the sample. A pair of observations (x_i, y_i) and (x_j, y_j) is said to be concordant if $(x_i - x_j)\,(y_i - y_j) > 0$, otherwise it is called discordant (Nelsen, 2006).

A rank correlation test verifies if $\hat{\tau}$ is statistically different from zero, i.e. if data are dependent. This index detects non linear dependencies, while the common Pearson's and Spearman's rho detect linear dependencies (Nelsen, 2006).

In the next Subsection, we explain how to obtain empirical copulas starting from data belonging to samples of first passage times (FPTs) or spike trains.

2.2. *Detect dependencies between ISIs through copulas*

Copulas are multivariate joint distributions. For this reason, they can be used to investigate dependencies in a neural network with n neurons. However, their use is more intuitive for $n=2$. The extension to the pairwise analysis for tn neurons is immediate, while the study of k dimensional dependencies, for $k=3,\dots,n$, is computationally not trivial, although it is theoretically analogous.

Given a sample $\{(X_1,Y_1),\dots,(X_n,Y_n)\}$, we calculate the empirical cdfs $\hat{F}$ and $\hat{G}$ as

$$\hat{F}(x) = \frac{1}{n}\sum_{i=1}^{n} 1_{\{X_i \le x\}}, \quad \hat{G}(y) = \frac{1}{n}\sum_{i=1}^{n} 1_{\{Y_i \le y\}}, \quad x, y \in \mathbb{R}. \tag{2}$$

Then, we define the pseudo-observations from the copula as $\hat{U}_i = \left(\hat{F}(X_i), \hat{G}(Y_i)\right)$, $i=1,\dots,n$. A scatterplot of $\hat{U}$, called "copula scatterplot", helps to understand dependencies between the involved rvs.

From the theory of copulas, we know that the points lying on the main diagonal (i.e. the diagonal which runs from the bottom left corner to the top right corner) correspond to times related by a strictly increasing function f such that $F(X)=fleft(G(Y))$. If $X \sim Y$, then f becomes the identity function, otherwise a new curve appears. Indeed, if the marginal distributions are different, then a straight line on the time scatterplot is transformed into a curve on the copula scatterplot. We call it *curve of monotony*. If X and Y are times, then the synchrony is caught by a straight line along the diagonal on the time scatterplot. These points are mapped into points lying on the main diagonal or on a curve on the copula scatterplot, depending on whether X and Y are identically distributed.

For independent rvs, characterized by the independent copula $C(u,v)=uv$, the scatterplot presents a uniform distribution of points on the square $[0,1]^2$. On the contrary, the presence of clusters of points reveals a specific dependency. Furthermore, we have considered the empirical cdf C_n and the empirical probability density function (pdf) C_n of the copula (Nelsen, 2006). Their study, together with the estimation of the Kendall's tau, gives further information about the dependencies between X and Y.

To illustrate how to apply copulas to neuronal data, we first assume to have a sample of FPTs $T=\{(T_A^1, T_B^1),\dots,(T_A^n, T_B^n)\}$, where (T_A^i, T_B^i) and (T_A^j, T_B^j) are independent for $i \neq j$ and $(T_A^i, T_B^i) \sim (T_A^j, T_B^j)$, where ~ denotes rvs with the same distributions. In this case, we can calculate the pseudo-observations as described before.

Then, to deal with pairs of spike trains, we need to define how to extract a sample of two-dimensional rvs, representative of the dependencies between the spike trains.Denote S_A^i and S_B^j the epochs of the i-th and the j-th events in the spike trains A and B, and T_A^i and T_B^j the i-th and j-th ISIs, for $i=1,\dots,n$; $j=1,\dots,l$. On a fixed time, the number of spikes of two neurons is different, i.e. $n \neq l$. We assume that the ISIs T_A^i (resp. T_B^j) in A (B) are independent and identically distributed and we denote them T_A (T_B).

To pursue the analysis, we select A as target neuron. To each spike time S_A^i, we associate the time θ^i, defined as the intertime between S_A^i and the first spike in B following it (Fig. 1, Panel I). The pairs $(T_A^1, \theta^1),\dots,(T_A^N, \theta^N)$ determine a sample (T_A, θ) for the study of the relationships between the spike trains. If the corresponding copula is not the independent copula, then there is a connection between the two neurons. We investigate it comparing the two scatterplots and testing if τ is statistically different from zero. Moreover, the copula scatterplot allows to make hypotheses on the dynamics driving the membrane potential (MP) evolutions of the two neurons, as explained in Section 4.

Another interesting task is the investigation of the duration (or "memory") of the dependency between spike trains. After a certain time M, neuron B may forget the activity of neuron A, if no new phenomena coupling their dynamics are present. The time M may be short, corresponding to instantaneous effect, or long, implying a durable effect in the coupling.

To investigate it, we consider the sample $\left(T_A, \theta + \sum_{k=1}^{m} T_B^{(k)}\right) = \left\{\left(T_A^1, \theta^1 + \sum_{k=1}^{m} T_B^{(1k)}\right),\dots,\left(T_A^{\tilde{N}}, \theta^{\tilde{N}} + \sum_{k=1}^{m} T_B^{(\tilde{N}k)}\right)\right\}$, as shown in Fig. 1, Panel I. Here, $T_B^{(ik)}$ corresponds to the k-th ISI following θ_i, while $\tilde{N}$ denotes the sample size that might change with m. In particular, we are interested in the value m such that the corresponding copula approaches the independent one, i.e. $\tau=0$. If the dependence disappears for small (large) m,

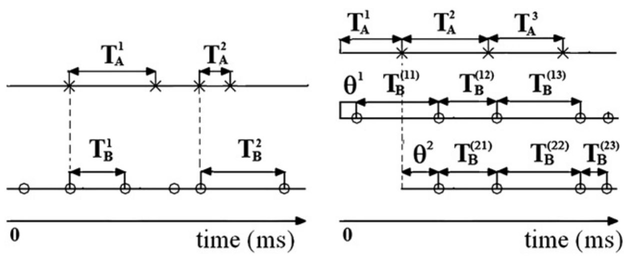

Fig. 1 – Samples of FPTs and of spike trains. Let A be the target neuron. Panel I: sample of FPTs, obtained considering only the first ISIs in A and B following synchronous spikes. Panel II: rvs involved in a sample of spike trains. For each T_A^i in A, we show the corresponding θ^i and the following $T_B^{(ik)}$ in B for $i=1$, 2 and $m=3$.

then the coupling has an instantaneous (long) effect. Furthermore, we study the optimal value m maximizing the coupling. It can be detected as the value of m that maximizes$\hat{\tau}$. Note that $m=0$ leads to the previous sample (T_A, θ).

To study the presence of delayed dependencies, we analyze the sample $(T_A, T_B^{(k)}) = \{(T_A^1, T_B^{(1k)}), \ldots, (T_A^n, T_B^{(nk)})\}$. Indeed, it might happen that a spike in A influences the k-th spike in B. Therefore, the delay can be estimated as $\theta + \sum_{j=1}^{k} T_B^{(ij)} - T_A^i$, where k is the first index such that the Kendall's tau for $(T_A, T_B^{(k)})$ is statistically different from zero.

These properties of memory and delayed dependencies hold when $\mathbb{E}[\theta + \sum_{i=1}^{k} T_B^{(i)}] - \mathbb{E}[T_A] > \mathbb{E}[T_B^{(k)}]$, i.e. the projection of $T_B^{(k)}$ on A does not overlap with T_A on average, otherwise such phenomena are due to the slower nature of A.

To conclude the analysis, we select B as target neuron and we repeat the procedure. Note that this is not necessary if T_A and T_B are identically distributed, since this leads to the same results, the study being symmetric.

3. Models for data generation

The samples were generated from two bivariate LIF models. Both of them describe the spike times of each neuron as the FPT of their MP evolution through a boundary, where the MPs are coupled through different rules.

3.1. *Model of the MP evolution through jump diffusion processes*

Musila and Lansky (1991) proposed to use jump diffusion processes to describe the MP evolution of a single neuron to account for the effects of the postsynaptic potentials (PSPs) impinging on the membrane near the trigger zone. Deco and Schürmann (1998) studied resonance phenomena for central neurons described by Ornstein Uhlenbeck (OU) processes with jumps modeling a discrete input spike train. In Sirovich (2003), jump processes are associated to the arrival of a spike, but the model is not a diffusion. Recently, Sirovich (2006) and Sirovich et al. (2007) proposed to use these processes to describe interactions in a small network.

Here, we describe the MP evolutions through a two dimensional jump diffusion process $\mathbf{X}(t) = \{(X_1, X_2)(t); t \geq t_0\}$. Each component evolves independently from the other, until the time when one of them attains a threshold value C for the first time. Then, that neuron releases a spike, its MP is reset to its resting value and the evolution restarts anew. Meanwhile, the MP of the other neuron has a jump of amplitude h (Fig. 2, Panel I) and then it pursues its evolution. In the absence of jumps, the MP of each neuron is modeled as an OU process given by

$$dX_i(t) = \left(-\frac{1}{\theta} X_i(t) + \mu_i\right) dt + \sigma_i dW_i(t), \tag{3}$$

with $t_0=0$ and $X_i(0)=x_{0i}$, for $i=1,2$. Here, τ, μ_i, σ_i denote the membrane constant (or decay time), the input and the noise intensity respectively. Moreover, $W_1(t)$ and $W_2(t)$ are two standard Wiener processes. Hence, the Brownian increments are independent.

We say that this corresponds to a local connection between neurons, since the dependency between spikes is direct, being determined only by the jumps.

To simulate a sample of FPTs T, we proceed as follows. When both neurons release a spike, the MPs are reset to their resting values and a new simulation starts. This type of sample reproduces the interspike times following synchronous spikes of the two neurons (Fig. 1, Panel I).

To generate two coupled spike trains, we collect the crossing times of the two MPs up to a maximum observed time t_{max}.

3.2. *Model of the MP evolution through correlated diffusion processes*

The Stein process for the spiking activity of a single neuron was introduced by Stein (1965). However, the study of the FPT problem for jump processes is mathematically intractable. Assuming the high frequency and the small amplitude of the jumps, diffusion limits have been proposed for instance by Capocelli and Ricciardi (1971) and Lansky (1984). From a

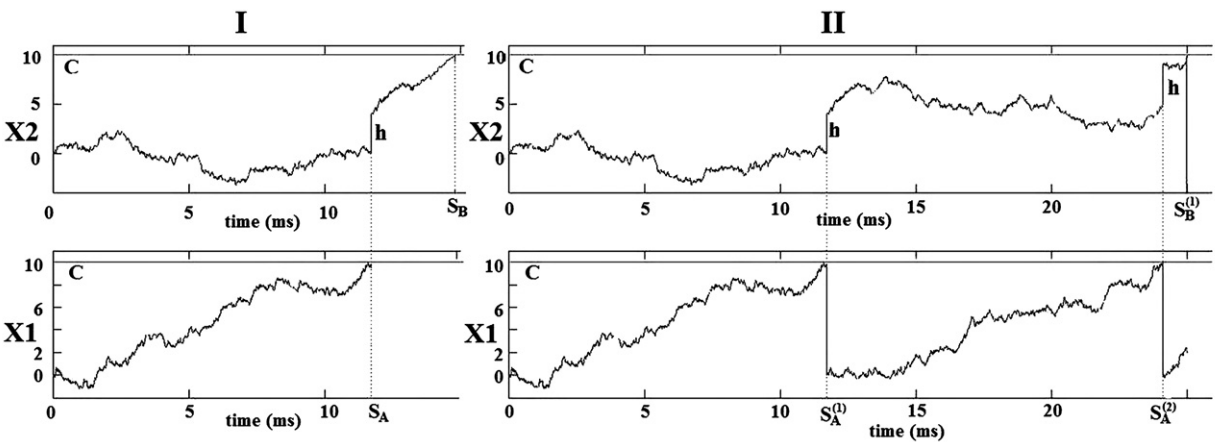

Fig. 2 – MP evolution through jump diffusion processes. Description of the MP evolution of two coupled neurons through a two dimensional jump process. The MP evolution of A (B) is reset to its resting value after that it spikes, meanwhile the MP evolution of B (A) has a jump of amplitude h. These dynamics are stopped when both neurons have released a spike (Panel I) or after a maximum time t_{max} (Panel II).

biological view point, when the neuron receives a huge number of inputs from the surrounding network, the continuous limit is a good approximation of the original process. A multivariate extension of these models has been recently proposed (Tamborrino et al., submitted for publication). There, the PSPs impinging on each neuron correspond to two kinds of input: those influencing a specific neuron and those simultaneously acting on a collection of at least two neurons.

Here, the MP evolutions of the two neurons are described by a bivariate diffusion process $\mathbf{X}(t)$ with correlated components. The sub-threshold MP evolutions are still described by Eq. (3), but now the Brownian increments are not independent anymore. Indeed, we assume $Cov(W_1(t),W_2(t))=\sigma_{12}t$, with $\sigma_{12}\in(0,1)$. Therefore, the evolutions proceed jointly in all the observed time intervals, due to the presence of a common noise. We say that this situation corresponds to a global kind of dependence, since the dependencies are determined by the surrounding network.

To obtain a sample of FPTs T, we stop the MP evolution of the fastest neuron after it fires. Meanwhile, the slowest one continues its evolution until its MP reaches the boundary (Fig. 3, Panel *I*). After that, the dynamics restarts anew. These neural dynamics are characterized by a continuous coupling effect up to the first spike.

To generate two coupled spike trains, we reset the MP of the firing neuron to its resting potential and then restart it. Meanwhile, the other neuron continues its evolution until it spikes (Fig. 3, Panel *II*). This procedure continues up to t_{max}, coupling the dynamics of the two neurons.

4. Results

In this Section, we apply our method on samples of FPTs and pairs of spike trains simulated from the jump and the covariance models. In Subsection 4.3, we enlighten the differences observed in the corresponding copula scatterplots. Performing the data analysis, we ignore the knowledge of the models and we infer coupling properties directly from copula scatterplots and Kendall's tau (values reported in the captions of the figures). The goodness of fit of the results is finally checked.

The parameter values of the models agree with those used for one dimensional LIF models in the literature. In particular, we choose membrane constant $\tau=10\,ms$, threshold value for the MP $C=10\,mV$, jump amplitude $h=3\ mV$, covariances 0.5; 0.8; 0.91 mV^2ms^{-1}, drifts and noise intensities are reported in Table 1. Examples of negative covariances, implying negative dependencies between spike trains, have been also analyzed, obtaining correct results. Also in this case, our method detects them. Unfortunately, the simulation of data from the jump model requests long computational times when we have negative jump amplitudes. For this reason, we do not illustrate these examples.

4.1. *Data from the jump model*

4.1.1. *Samples of FPTs*

The biological interpretation of samples of FPTs is not intuitive, since they do not correspond to time series. However, they can be interpreted as the intertimes after synchronous spikes (Fig. 1, Panel *I*) and their analysis helps to understand the use of copula scatterplots.

In Fig. 4, we report the copula scatterplots for different samples of T, obtained from the jump model, using the parameters reported in Table 1, with $h=3\,mV$. We first test the null hypothesis H_0:$T_A\sim T_B$ through a Kolmogorov–Smirnov (KS) test. Since the p-values $\hat{P}$ are 1, 0.998, 0.901 and 0 respectively, we reject H_0:$T_A\sim T_B$ only for the fourth sample, in agreement with how they were sampled.

We start considering the first three samples. The distribution of T_A (and hence of T_B) changes in each sample. Indeed, their means and variances are different (values not reported).

From the scatterplots and the values of $\hat{\tau}$ in Fig. 4, Panels *I–III*, we observe the following features:

1. Panels are characterized by decreasing values of $\hat{\tau}$, all statistically different from 0.
2. many points lie on the main diagonal, drawing its shape;

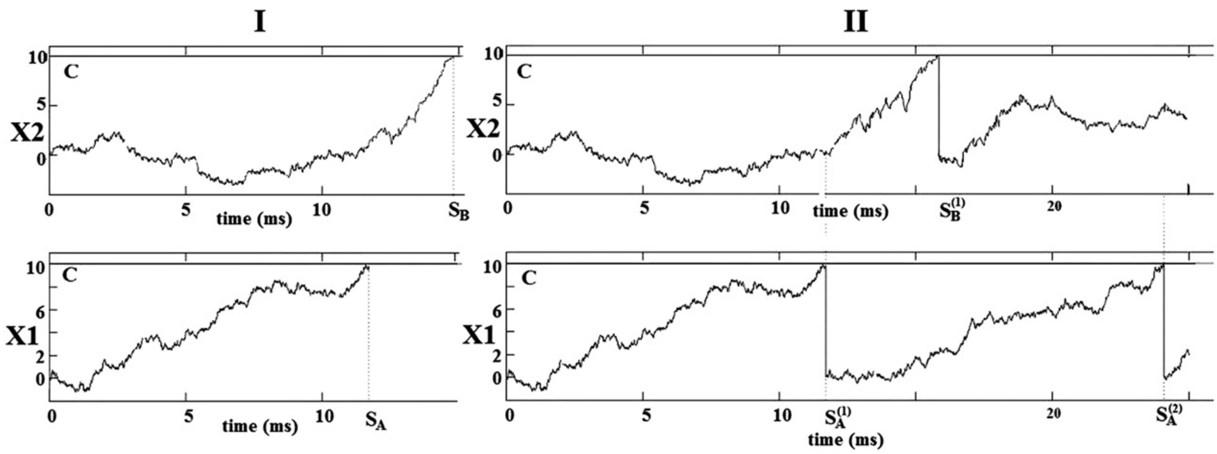

Fig. 3 – MP evolution through correlated diffusion processes. Example of MP evolution of two neurons coupled through a two dimensional correlated diffusion process. The MP evolution of *A* (*B*) is reset to its resting value after it spikes, while the MP evolution of *B* (*A*) is not influenced by the spike. These dynamics are stopped after both neurons have released a spike (Panel I) or after a maximum time t_{max} (Panel II).

Table 1 – Drifts μ and noise intensities σ^2 used to simulate spike data. Units are: $mVms^{-1}$ and mV^2ms^{-1}, respectively.

Case	μ_A	μ_B	σ_A^2	σ_B^2
I	1.2	1.2	0.3	0.3
II	1.2	1.2	0.5	0.5
III	1.2	1.2	1.1	1.1
IV	1.0	1.5	0.5	0.5

3. scatterplots exhibit similar features, although with different densities of the points. Moving from the left to the right side, the density of the points not on the diagonal increases;
4. there is a lack of points around the main diagonal.

Due to feature 1, a dependency is caught by the method in each sample. The analogies between the plots suggest the presence of a similar coupling phenomenon acting with different strengths, as suggested also by the first feature. The coupling phenomenon acts only to determine the synchrony, while the other intertimes are scarcely dependent. Indeed, feature 4 and the lack of clusters do not reveal further dependencies. That means that specific phenomenon might determine synchronous spikes or have no effect if the instantaneous coupling is not strong enough. A local connection is compatible with this kind of behavior. These remarks agree with the underlying model used to generate the samples.

Now, consider Panel *IV*. Also in this case, a positive $\hat{\tau}$ is observed, but the copula scatterplot is not symmetric anymore. In the time scatterplots (figures not reported), we observe many points lying on the main diagonal. Therefore, the curve in Panel *IV* corresponds to the curve of synchrony. Moreover, a high density of points is observed on the curve that is surrounded by a lack of points. Hence, we can hypothesize a similar dynamics to that observed in Panels *I–III*, but with different marginals.

4.1.2. *Samples of spike trains*

We consider two spike trains generated according to the jump model with parameters given by case *III* in Table 1. We cannot reject H_0: $T_A \sim T_B$, since $\hat{p} = 0.998$. Therefore, the analysis does not change inverting the roles of target and reference neurons. Thus, we choose *A* as target neuron.

The pairs $(T_A, T_B^{(k)})$ are characterized by Kendall's tau statistically equal to zero (e.g. $\hat{p} = 0.71, 0.70, 0.79$ for $k = 1,2,3$). Hence, the samples do not present delayed coupling phenomena.

In Fig. 5, we report the copula scatterplots of $(T_A, \theta + \sum_{k=1}^{m} T_B^{(k)})$ for $m = 0,1,2,3,5,10$. From these plots and the values of $\hat{\tau}$, we observe that increasing the value of *m*, the copula scatterplots approach the independent copula.

In Panel *I*, the curve with the highest density of points is well approximated by a straight line. Moreover, T_A and θ have a similar distribution (histograms not shown). Since $T_A \sim T_B$, θ, and T_B have a similar distribution too. Therefore, the spiking dynamics are characterized by the presence of synchronous spikes. Moreover, we observe a lack of points around the diagonal, as in Fig. 4. Therefore, we can hypothesize a local coupling.

In the remaining panels, new curves catch the dependency between T_A and $\theta + \sum_{k=1}^{m} T_B^{(k)}$. Since these rvs have different distributions (p-values not reported), these curves correspond to curves of monotony.

Now, we consider two spike trains obtained with parameters of case *IV* in Table 1. We reject H_0:$T_A \sim T_B$ and H_0:$T_A \sim \theta$, since both p-values are null. The Kendall's tau for $(T_A, T_B^{(k)})$ is statistically different from zero only when $k = 1$, since $\hat{p} \approx 0$ for H_0: $\tau = 0$. However, it does not represent a delayed dependency, since $\mathbb{E}[T_A] = 17.92$, $\mathbb{E}[\theta + T_B^{(1)}] = 20.40$ and $\mathbb{E}[T_B^{(1)}] = 10.32$.

In Fig. 6, we plot the copulas for $(T_A, \theta + \sum_{k=1}^{m} T_B^{(k)})$. Here, $m = 1$ maximizes $\hat{\tau}$. This figure presents some similarities to Fig. 5. Indeed, for *m* greater than the optimal one, the dependency decreases and the copula scatterplots look like the independent copula. Moreover, in both figures, we observe a lack of points around the curve of monotony for $m = 0$ and 1 as well as the presence of clusters. Finally, in Fig. 6, these curves can be detected up to $m = 5$.

The analogies between samples of Figs. 5 and 6 allow to hypothesize dynamics for the spike trains driven by similar kinds of dependencies, even if with different marginal behaviors.

Since T_A and T_B are not identically distributed, we repeat the analysis considering *B* as target neuron. In Fig. 7, we report the copula scatterplots for $m = 0, 1, 2$. The shapes of these scatterplots and the strength of the dependencies caught by $\hat{\tau}$ are different from those in Fig. 6. Also in this case, $\hat{\tau}$ is statistically different from 0. Furthermore, a curve of monotony is

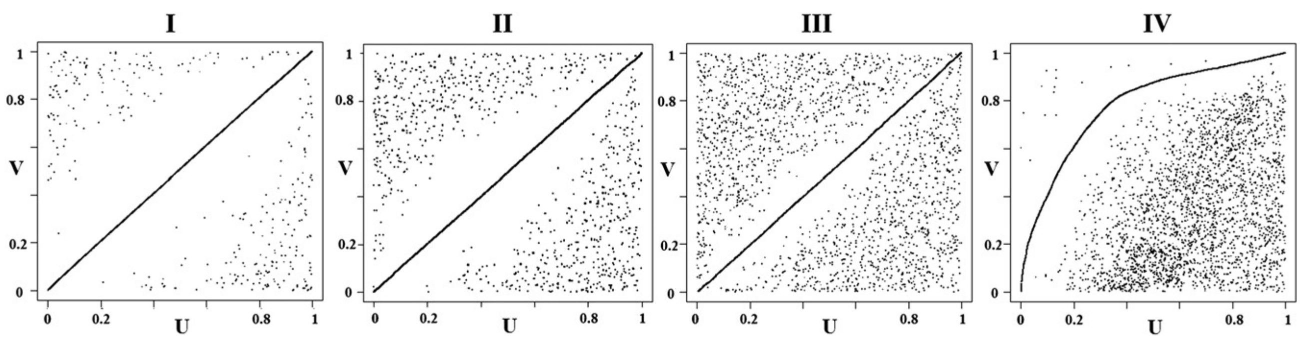

Fig. 4 – Samples of FPTs from the jump model. Copula scatterplots corresponding to four samples of ISIs (T_A, T_B), where $T_A \sim T_B$ for the first three pairs. The estimated Kendall's tau are $\hat{\tau}_I$–0.84, $\hat{\tau}_{II} = 0.69$, $\hat{\tau}_{III} = 0.41$ and $\hat{\tau}_{IV} = 0.18$, respectively. They are statistically different from zero, since all the corresponding p-values are smaller than 0.05.

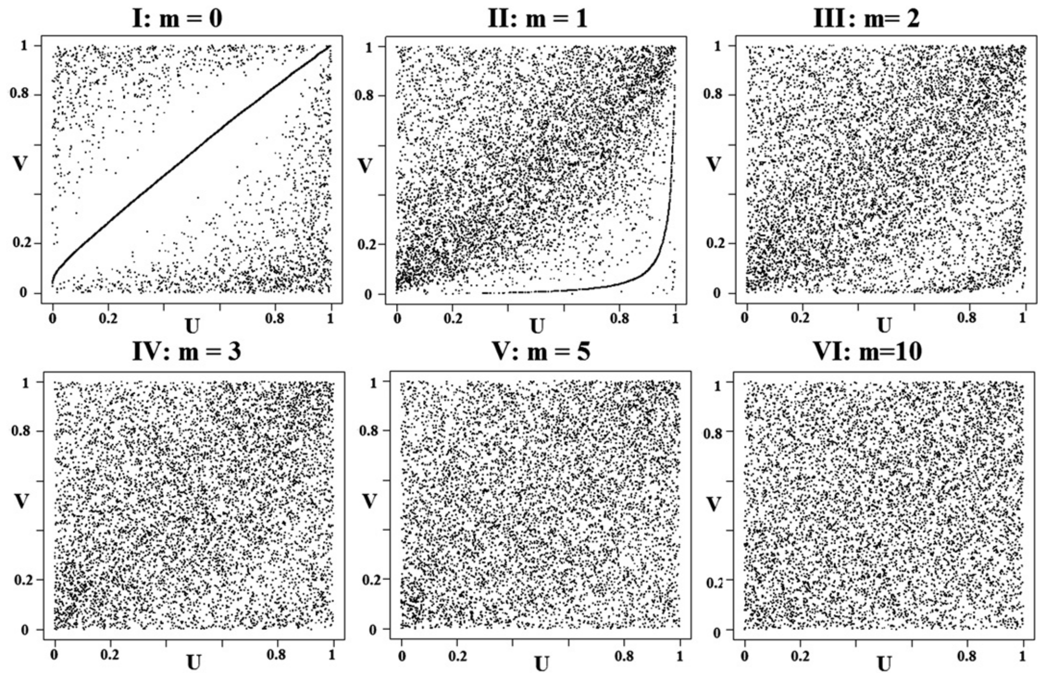

Fig. 5 – Sample of spike trains from the jump model, where $T_A \sim T_B$. Copula scatterplots of $(T_A, \theta+\sum_{k=1}^{m} T_B^{(k)})$, for m = 0, 1, 2, 3, 5, 10, where T_A and T_B have the same distribution. The estimated Kendall's tau are statistically different from zero, with values $\hat{\tau}_I = 0.42, \hat{\tau}_{II} = 0.20, \hat{\tau}_{III} = 0.15, \hat{\tau}_{IV} = 0.12, \hat{\tau}_V = 0.10$ and $\hat{\tau}_{VI} = 0.07$, respectively. Note that $m = 0$ represents the optimal value maximizing the dependency between the involved times.

recognized only for $m = 0$. This is related to the slower nature of neuron *A*.Note that we have detected dependencies alternating *A* and *B* as target neurons. Therefore, there exists a bi-directional influence connection between the two neurons.

The results obtained applying our method are coherent with the features of the models used to simulate data. In particular, we were able to detect bi-directional connections, such as those determined by the jump dynamics of the

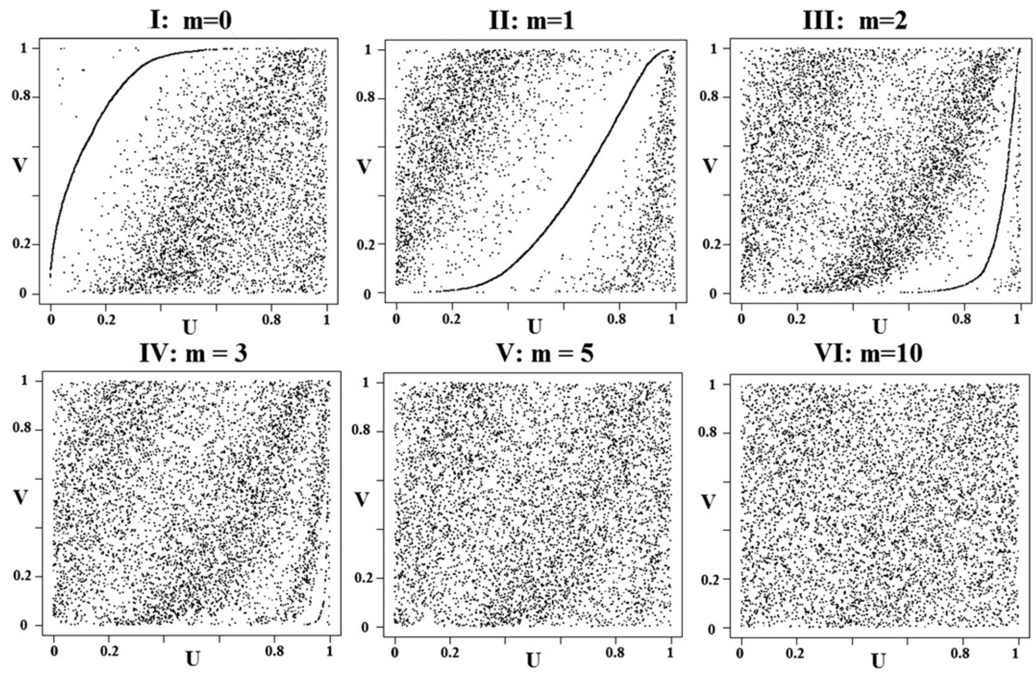

Fig. 6 – Sample of spike trains from the jump model with different distributions of T_A and T_B. Copula scatterplots of $(T_A, \theta+\sum_{k=1}^{m} T_B^{(m)})$, for m = 0, 1, 2, 3, 5, 10, where T_A and T_B have different distributions. The estimated Kendall's tau are statistically different from zero and equal to $\hat{\tau}_I = 0.04, \hat{\tau}_{II} = 0.12, \hat{\tau}_{III} = 0.06, \hat{\tau}_{IV} = 0.04, \hat{\tau}_V = 0.02, \hat{\tau}_{VI} = 0.01$, where $m = 1$ represents the optimal value maximizing $\hat{\tau}$.

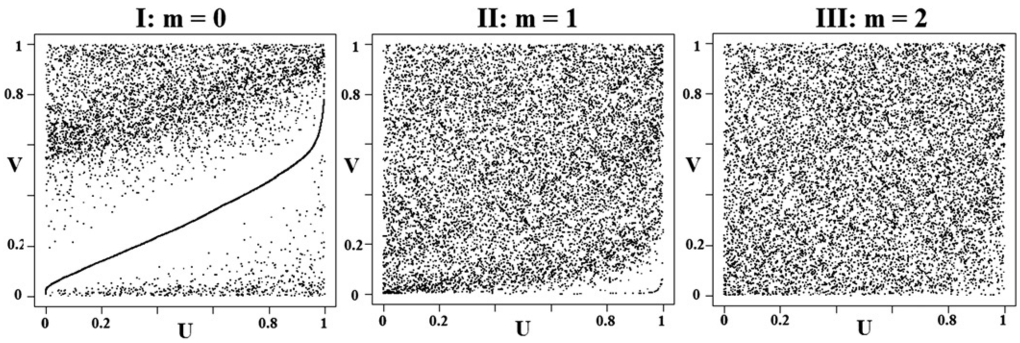

Fig. 7 – Choice of B as target neuron. Copula scatterplots of ($T_B, \theta+\sum_{k=1}^{m} T_A^{(k)}$), for m=0, 1, 2, obtained considering B as target neuron in the spike trains analyzed in Fig. 6. The estimated Kendall's tau are $\hat{\tau}_I = 0.23, \hat{\tau}_{II} = 0.08, \hat{\tau}_{III} = 0.06$, respectively. The maximum dependence is observed for m=0.

considered model, as well as to hypothesize a correct local coupling. As previously remarked, we have ignored the knowledge of the underlying models during the analysis phase.

4.2. *Data from the covariance model*

Here, we consider data generated from the covariance model with parameters reported in Table 1 and covariances equal to 0.5, 0.8, 0.91, 0.8 mV^2ms^{-1}, respectively.

4.2.1. *Samples of FPTs*

In Fig. 8, we report the copula scatterplots coming for the four samples of FPTs. Testing H_0: $T_A \sim T_B$, we obtain $\hat{p} = 0.69$, 0.95, 0.89 and 0, respectively. We start considering the first three pairs, characterized by identically distributed ISIs.

Looking at Fig. 8, Panels *I–III* and the corresponding $\hat{\tau}$, we observe the following features:

1. Panels are characterized by increasing values of $\hat{\tau}$, all statistically different from 0.
2. many points lie on the main diagonal and around it;
3. scatterplots exhibit similar features, although with different densities of the points. Moving from the left to the right side, the density of the points far from the diagonal decreases.

Positive dependencies are caught in all samples. Furthermore, the numerous points lying on the diagonal (indicator of synchrony) are surrounded by a cloud of other points. This suggests the presence of a noise that continuously perturbs the coupling phenomenon, destroying the synchrony. A global connection is compatible with this kind of behavior.

Now, consider Panel *IV*. In the time scatter plot, not reported, (resp. copula scatterplot) no points lie on or above the main diagonal (the curve of synchrony), due to the fact that $\mathbb{E}[T_A] = 24.98$, $\mathbb{E}[T_B] = 10.65$. Therefore, no synchrony is observed. For the similarity with Panel *I*, we hypothesize a similar dynamics characterized by different marginals.

4.2.2. *Samples of spike trains*

We consider two spike trains generated with drifts and variances given by case *III* in Table 1, and covariance 0.91 mV^2ms^{-1}. We cannot reject $T_A \sim T_B$, since $\hat{p} = 0.94$. Therefore, it is sufficient to consider *A* as target neuron.

In Fig. 9, we report the copula scatterplots of ($T_A, \theta+\sum_{k=1}^{m} T_B^{(k)}$) for m=0, 1, 2, 3, 5, 10. From these plots and the values of $\hat{\tau}$, we note that the copula scatterplots approach the independent copula as m increases.

In Panel *I*, T_A and θ have different distributions since $\hat{p} = 0$ for the hypothesis H_0: $T_A \sim \theta$. Therefore, the monotone dependency is caught by a curve and the largest part of the points lays on and under it. This behavior may be explained admitting the existence of a noise that perturbs the system and destroys the deterministic relationship. Furthermore, the dependencies seem to be determined by a continuous phenomenon that tunes the activity of the two neurons, despite

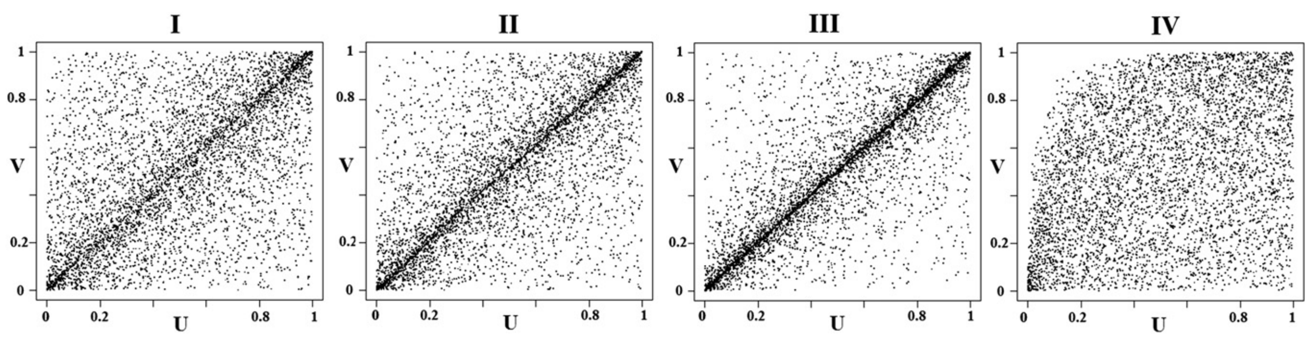

Fig. 8 – Samples of FPTs from the covariance model. Copula scatterplots corresponding to four pairs of ISIs (T_A,T_B), with $T_A \sim T_B$ for the first three pairs. The estimated Kendall's tau are $\hat{\tau}_I = 0.41, \hat{\tau}_{II} = 0.53, \hat{\tau}_{III} = 0.67$, respectively. They are statistically different from zero, since the corresponding p-values are smaller than 0.05.

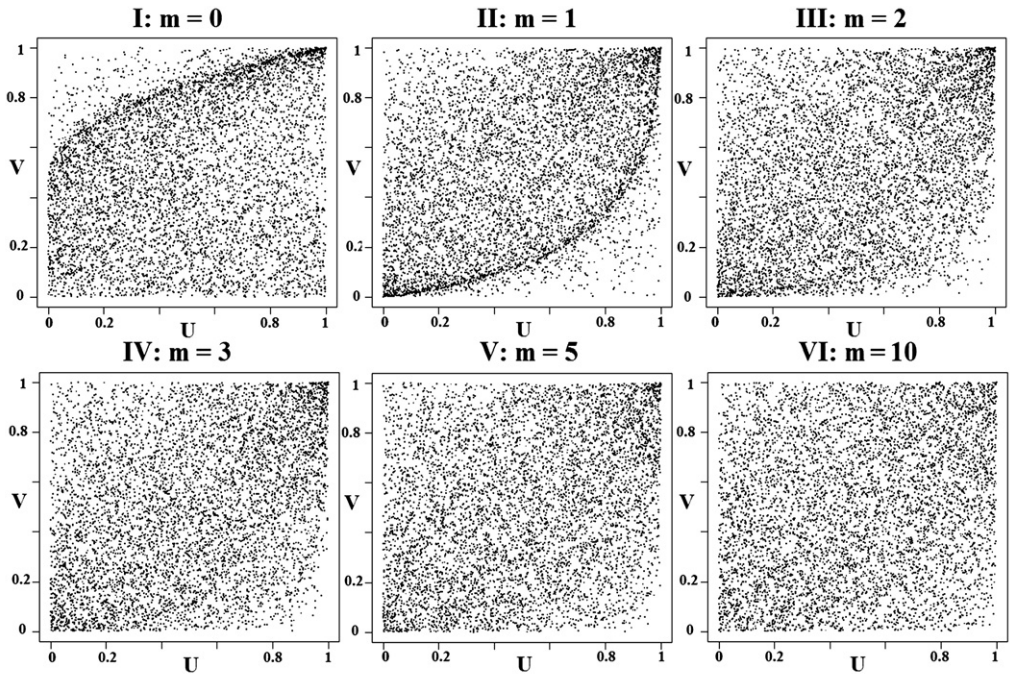

Fig. 9 – Sample of spike trains from the covariance model, where $T_A \sim T_B$. Copula scatterplots of $(T_A, \theta + \sum_{k=1}^{m} T_B^{(k)})$, for $m=0$, 1, 2, 3, 5, 10, where T_A and T_B have the same distribution. The estimated Kendall's tau are statistically different from zero, with values $\hat{\tau}_I = 0.16$, $\hat{\tau}_{II} = 0.30$, $\hat{\tau}_{III} = 0.25$, $\hat{\tau}_{IV} = 0.22$, $\hat{\tau}_V = 0.18$, and $\hat{\tau}_{VI} = 0.14$, respectively. Note that $m=0$ represents the optimal value maximizing the dependency between the involved times.

the noise. Therefore, a global coupling might be hypothesized. This is supported by the fact that $(T_A, \sum_{k=1}^{m} T_B^{(k)})$ becomes statistically independent for $m \geq 409$. That means that we are observing a long memory phenomenon.

In the remaining panels, new curves of monotony catch the synchrony between T_A and $\theta + \sum_{k=1}^{m} T_B^{(k)}$. In particular, in Panel *II*, the number of points lying on this curve is greater than those in Panel *I*.

Finally, we consider two spike trains generated using the parameters given by case *IV* in Table 1, and covariance $0.8\, mV^2 ms^{-1}$. We reject H_0: $T_A \sim T_B$, since $\hat{p} \approx 0$. In Fig. 10, we plot the copulas for $(T_A, \theta + \sum_{k=1}^{m} T_B^{(k)})$. Here, $m=2$ maximizes $\hat{\tau}$ for the considered samples and curve of monotony can be detected up to $m=5$. This figure presents some similarities to Fig. 9. Indeed, for m greater than the optimal value, the dependence decreases and the copula scatterplots look like the independent copula. These analogies allow to hypothesize dynamics for the spike trains driven by similar kinds of dependencies, even with different marginal behaviors.

Due to the different roles of neurons *A* and *B*, we repeat the analysis considering *B* as target neuron. The copula scatterplots for $m=0$, 1, 2 are plotted in Fig. 11. The shapes are obviously different from those in Fig. 10, but also in this case, $\hat{\tau}$ is statistically different from 0. Therefore, we have detected a bi-directional connection between the two neurons.

In both samples, no delayed phenomena are detected. Indeed, no p-values statistically different from zero are observed for $(T_A, T_B^{(k)})$ such that $\mathbb{E}[\theta + \sum_{i=1}^{k} T_B^{(i)}] - \mathbb{E}[T_A] > \mathbb{E}[T_B^{(k)}]$.

The results agree with those expected, determined by the structure of the used model.

4.3. *Comparison between data from the two models*

Data used in Figs. 4–8, 5–9, 6–10, 7–11 came from two OU processes with the same parameters, but coupled according to different rules, i.e. jumps or positive covariances. The different coupling leads to different shapes in the copula scatterplots, as well as to different properties. For instance, copula scatterplots related to the jump model are characterized by a lack of points around the main diagonals, while a cluster of points is observed in those coming from the covariance model. This allows us to hypothesize different coupling phenomena for those scatterplots presenting different features.

Furthermore, we may observe different shapes of scatterplots even with a similar $\hat{\tau}$. Look for instance at Fig. 4, Panel *II* and Fig. 8, Panel *III*, with $\hat{\tau} = 0.69$ and $\hat{\tau} = 0.67$, respectively. Therefore, the study of correlation or rank correlation indexes, such as the Pearson's rho or the Kendall's tau, is useful to recognize the presence of dependencies, but it cannot be used to investigate their nature.

5. Discussion

The use of copulas allows a new approach to analyze dependencies between spike trains. The discussed examples illustrate some features highlighted by means of this technique. Suitable statistical tests and further developments of the mathematical tools will allow to determine families of copulas able to fit data. Furthermore, a classification of the

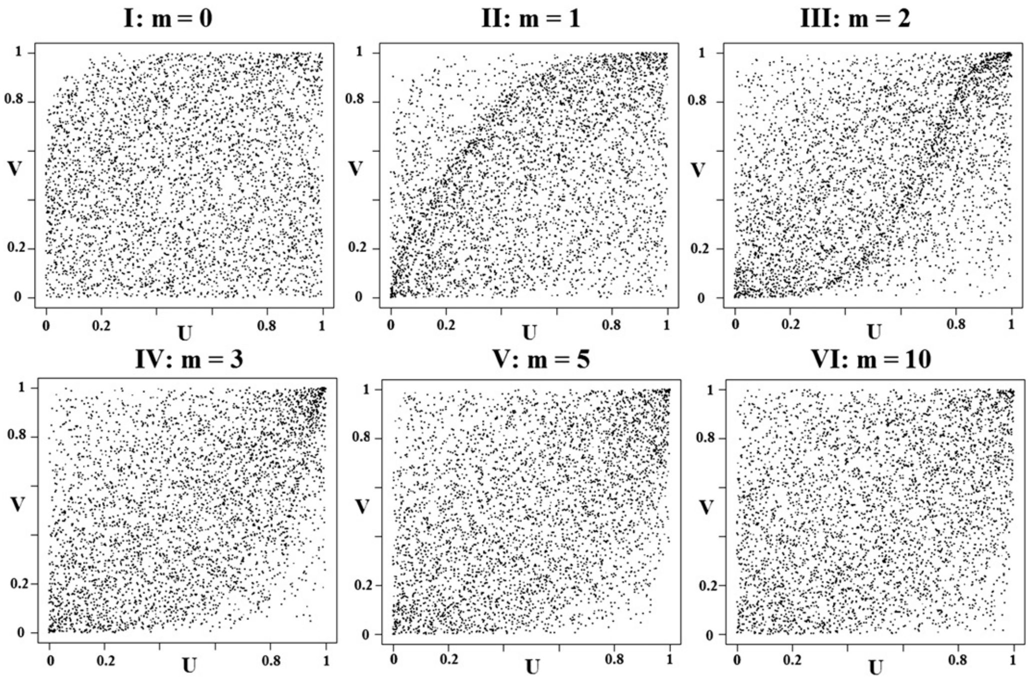

Fig. 10 – Sample of spike trains from the covariance model, with different distributions of T_A and T_B. Copula scatterplots of $(T_A, \theta+\sum_{k=1}^{m} T_B^{(m)})$, for m = 0, 1, 2, 3, 5, 10, where T_A and T_B have different distributions. The estimated Kendall's tau are statistically different from zero and equal to $\hat{\tau}_I = 0.07, \hat{\tau}_{II} = 0.27, \hat{\tau}_{III} = 0.33, \hat{\tau}_{IV} = 0.31, \hat{\tau}_V = 0.26, \hat{\tau}_{VI} = 0.20$, where m = 2 represents the optimal value maximizing τ.

different copulas corresponding to different kinds of coupling may help to interpret the structure of the network.

In this Section, we compare some of our results with those obtained through classical tools. At first, we consider crosscorrelograms and time scatterplots. Then, we briefly discuss some features of the GLMs and finally we perform a detailed comparison with the Cox method.

Crosscorrelograms are one of the most used techniques to analyze spike trains. They detect synchronous and delayed activities but they are often unable to recognize other kinds of dependencies. Reversely, in copula scatterplots, the layout of the points out of the curve of synchrony discloses the presence of other kinds of dependencies. Moreover, it helps to hypothesize the underlying coupling effects. A common feature between crosscorrelograms and the proposed approach is the necessity to fix a target neuron. Usually, the analysis is repeated, exchanging the roles of the two neurons.

The analysis of crosscorrelograms requests the simultaneous study of the autocorrelograms. Indeed, oscillations in the crosscorrelogram might be due to marginal behaviors, as described by Sacerdote and Tamborrino (2010) and Tetzlaff et al. (2008). Thus, it is not always possible to distinguish between the two cases. Furthermore, the duration of the dependencies is hidden in crosscorrelograms. Indeed, this information depends on the presence of several peaks or troughs and by their width. Unfortunately, these features

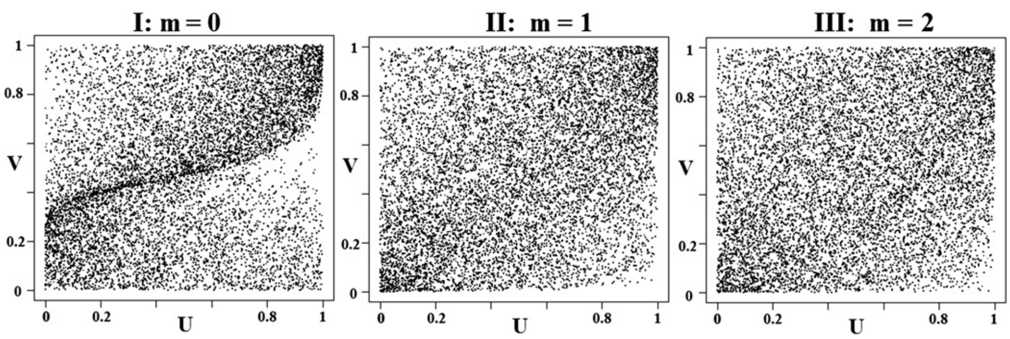

Fig. 11 – Choice of B as target neuron. Copula scatterplots of $(T_B, \theta+\sum_{k=1}^{m} T_A^{(k)})$, for m = 0, 1, 2, obtained considering B as target neuron, in the spike trains analyzed in Fig. 10. The estimated Kendall's tau are $\hat{\tau}_I = 0.27, \hat{\tau}_{II} = 0.22, \hat{\tau}_{III} = 0.18$ and m = 0 maximizes the dependency.

change according to the used bin. On the contrary, copulas allow to determine the value of m such that the two considered random times become independent, disclosing memory properties. In Fig. 12, we show autocorrelograms and crosscorrelograms corresponding to samples analyzed in Figs. 5 and 9. For each sample, we only plot one autocorrelogram, since $T_A \sim T_B$. In the crosscorrelograms, peaks and troughs far from zero are due to the marginal behaviors, as explained by the autocorrelograms. Hence, these oscillations do not represent two neurons firing with a delay, i.e. the only statistically meaningful peaks are those in 0.

One might wonder why to use copula scatterplots instead of time scatterplots. In a time scatterplot, one can easily recognize synchronous spikes from the presence of a straight line. Furthermore, such plot gives information on the marginal behavior, allowing to recognize the range of the involved times. However, the merge of marginal and joint behaviors represents the main limit of this tool. Indeed, it is hard to distinguish meaningful clusters, observing clouds of points (Fig. 13, Panels *I* and *IV*). Hence, any classification of the observed kinds of dependencies becomes difficult. Reversely, copula scatterplots (Fig. 13, Insets *I′* and *IV′*) solve this problem, catching only the joint behavior, since the marginal distributions are uniform. The same considerations hold when one plots the 3-D histograms for the times (Fig. 13, Panels *II* and *V*) and for the copulas (Fig. 13, Panels *III* and *VI*).

GLMs, as well as correlation indices, privilege linear dependencies, while copulas and the Kendall's τ deal with any kind of dependency. For instance, correlation indices assume value 1 when the rvs are related by a linear relationship. On the contrary, the Kendall's tau is equal to 1 if there exists a strictly increasing transformation between the rvs. Furthermore, GLMs are sensible to the amplitude of the test window. In our approach, this problem becomes relevant only plotting a 3-D histogram for the copula, to perform a fit of data to a specific family of copulas.

The recent upgrading of the Cox method makes it a useful approach for the detection of dependencies in a neural network (Masud and Borisyuk, 2011). They study the dependency of a target neuron A on the other $(n-1)$ reference neurons, considering pairwise dependencies. For this reason, we focus on the comparison of the two methods for the case $n-2$, reporting the main advantages of each method.

5.1. *Copula method versus Cox method*

5.1.1. *The Cox method*

The Cox method makes use of the hazard function, that is defined as the occurrence rate at time t conditional on survival time until time t or later:

$$\varphi(t) = \lim_{\Delta t \to 0} \frac{P(t \le T \le t + \Delta t | T > t)}{\Delta t} = \frac{f(t)}{1 - F(t)}.$$

Here, $F(t)$ is the cdf of the ISIs and $f(t)$ is their density.

In (Masud and Borisyuk, 2011), modulated renewal processes (refer to Cox (1972) and Borisyuk et al. (1985)) have been considered to introduce the dependency between spike trains. They suppose that the hazard function ϕ of the target neuron A is a product of two multipliers. The first term is the hazard function φ of the renewal process A without influence from the reference neuron B, and the second term describes the influence of neuron B on A. In particular, they introduce an influence function $Z_B(t)$ that determines how the reference neuron influences the target. They propose to use a hazard function given by

$$\varphi(t) = \varphi_A(U_A(t)) \exp(\beta Z_B(t)). \tag{4}$$

Here, $U_A(t)$ is the backward recurrence time of the process A at time t and β is the parameter that has to be estimated (Perkel et al., 1967). It gives the strength of influence from train B to A: if $\beta-0$, no influence is observed. Their method provides an estimation of β and a confidence interval for the test hypothesis H_0:$\beta-0$.

As influence function Z_B, they choose the alpha function proposed by Gerstner and Kistler (2002) to describe the synaptic connectivity between neurons. This choice implies the necessity to estimate a set of parameters: the delay time Δ due to spike propagation from neuron B to A and the characteristic decay and rise times of the postsynaptic potential (PSP), denoted by τ_s and τ_r, respectively.

The estimation of Δ can be properly done using using a pairwise Cox method or considering the time shift to the right side of zero corresponding to the highest value of the crosscorrelation function exceeding the upper boundary. If the MP evolution is described by a Stein's model, the decay time can be estimated

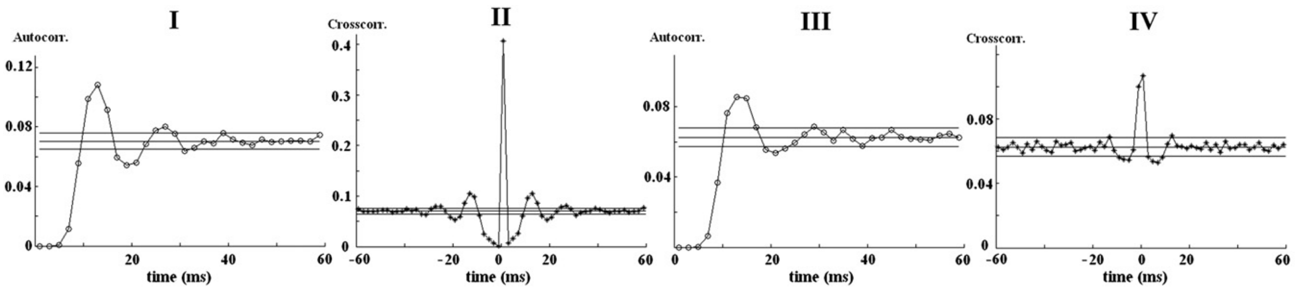

Fig. 12 – Autocorrelograms and crosscorrelograms. Panels *I* and *III*: autocorrelograms of TA for the samples analyzed in Figs. 5 and 9, respectively. The line with circles represents the estimated autocorrelation. The two straight lines limit the confidence interval at 0.05 for $\frac{1}{\mathbb{E}[T_A]}$. Panels *II* and *IV*: crosscorrelograms for the considered samples. The line with stars (dotted line) denotes the empirical (theoretical) crosscorrelation, while the two straight lines delimit a confidence interval for the hypothesis of independence between T_A and T_B.

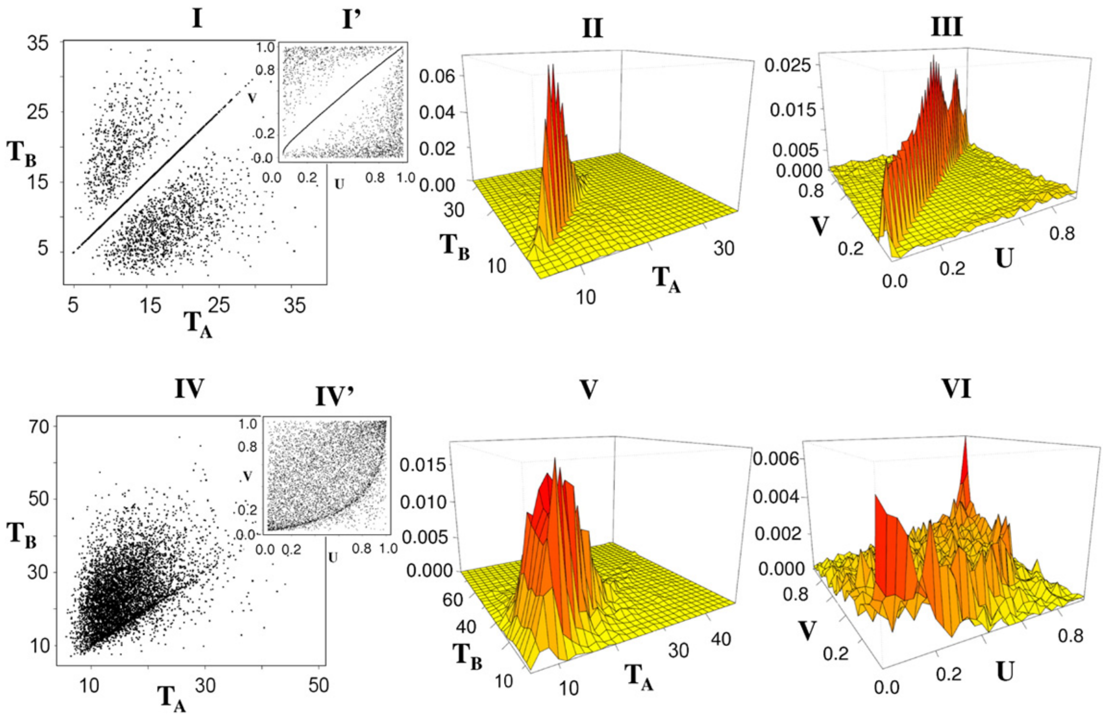

Fig. 13 – Analyses through ISIs and copulas. Scatterplots and 3-D histograms for times and copulas. The upper (lower) panels correspond to the samples analyzed in Fig. 5 (Fig. 9). Panels *I*, *IV*: ISI scatterplots of (T_A,T_B). Inset *I'*: copula scatterplot corresponding to (T_A,θ) (previously shown in Fig. 5, Panel *I*). Panel *IV'*: copula scatterplot corresponding to (T_A, $\theta+T_B^{(1)}$) (already shown in Fig. 9, Panel *II*). Panels *II* and *V*: 3-D time histograms. Panels *III* and *VI*: 3-D copula histograms.

from the ISI data using the algorithm in Tuckwell and Richter (1978), while the rise time is assumed to satisfy $\tau_s = \frac{1}{100}\tau_r$.

In general, the estimation of τ_s and τ_r from the ISI data is an unsolved task. Indeed, it requires the knowledge of the underlying model and the measurement of the PSP. Therefore, the results from the method may become unreliable. A solution might be to change the influence function Z_B, choosing a more general expression.

In the sequel, we consider a set of examples analyzed with the two methods.

5.1.2. *Examples*

We apply the Cox method to the data sample used in Section 4. For an OU process, $\tau_s=\theta$, while $\tau_s=\theta$. However, to perform the analysis, we assume $\tau_r=0.1$, as in Masud and Borisyuk (2011). The delay Δ is estimated using crosscorrelograms. To estimate β from Eq. (4) and its confidence interval, we use the software provided kindly to us by Borisyuk and Masud.

Using data from the covariance model, we obtain $\Delta=0$ or $\Delta=1$. With these estimates, the Cox method correctly catches the bi-directional dependencies, providing statistically positive estimates of β (analysis not reported).

However, the method does not succeed using data from the jump model. Choosing *A* as target neuron, we investigate β_{BA}, i.e. the influence from *B* to *A*. Here, we report the study of the Cox method on the spike trains analyzed in Fig. 5, with crosscorrelogram in Fig. 12, Panel *II*. Looking to the right side of Fig. 12, two peaks are observed at times 0 and 10. However, the second one is due to the autocorrelation and therefore, we choose $\Delta=0$. This leads to $\beta_{BA}=-5.89$ with confidence interval $(-6.22;-5.59)$. Therefore, a wrong negative dependency is caught. Vice versa, choosing the wrong delay $\Delta=10$, we got a correct positive dependency $\beta_{BA}=0.71$, with confidence interval $(0.46;0.97)$. Choosing *B* as target neuron, similar features follow (data not reported).

Hence, the goodness of the results depends highly on the underlying model and on the ability of the experimenter to estimate the parameters correctly, when this can be done, i.e. when we can measure the PSP or we know τ_r and τ_s in advance.

As a second check, we have generated two spike trains according to the enhanced LIF model described in (Borisyuk, 2004), using the software from the website www.tech.plymouth.ac.uk/infovis. This model considers different biological parameters, e.g. the already mentioned Δ and τ_s, but also the absolute refractory period *r*, defined as the interval following a spike where the neuron is unable to spike again. Furthermore, the software allows to specify the connection scheme between the two neurons.

Here, we test the Copula method on two spike trains generated choosing $\Delta=7, \tau_s=2.78, \tau_r=0.1, r=5$ and uni-directional connection $\beta_{BA}=12.18$, i.e. *B* influences *A*. Choosing *A* as target neuron, no delayed phenomena are observed. Indeed, the Kendall's tau for the pairs $(T_A, T_B^{(k)})$ are statistically equal to zero (refer to Table 2, for k=1, 2). Reversely, we obtain a positive Kendall's tau for $m=0$, i.e. for the pair (T_A,θ). Furthermore, the pairs $(T_A, \theta+\sum_{k=1}^{m} T_B^{(k)})$ are independent for $m>1$, having a p-value larger than 0.05 (values not reported). Therefore, these data are characterized by an instantaneous effect. Choosing *B* as target neuron, no dependencies are catched, as shown in Table 2. Hence, as the Cox method, our method catches the connection scheme correctly.

Table 2 – Kendall's tau from different pairs of rvs extracted from spike trains generated via the enhanced LIF model. The choice of A as target neuron leads to a positive dependence between (T_A, θ). Vice versa, selecting B as target neuron, no dependencies are observed. Therefore, a uni-directional connection is found.

A as target neuron			B as target neuron		
Case	$\hat{\tau}$	p-value	Case	$\hat{\tau}$	p-value
$(T_A, T_B^{(1)})$	−0.0094	0.4862	$(T_A, T_B^{(1)})$	0.0307	0.0538
$(T_A, T_B^{(2)})$	−0.0038	0.7807	$(T_B, T_A^{(2)})$	0.0074	0.6407
(T_A, θ)	0.0527	0.0001	(T_B, θ)	0.0092	0.5672

5.1.3. *Advantages of the two methods*

Summarizing, each method presents some advantages and disadvantages, according to different situations.

The main advantages of the copula method are that:

- it is a non parametric method, only requesting the renewal assumptions, i.e. iid ISIs;
- it recognizes the duration of the effect of a coupling phenomenon through the investigation of m;
- it allows to recognize the presence of similar underlying dynamics for the MP, when the copula scatterplots or densities have similar shapes;
- it gives the possibility to fit the joint distribution for the examined ISIs, after a fit of the copula density. This allows a classification of different kinds of dependencies (not present in this paper);
- it might be extended to capture dependencies in triplets, quartets, etc.

A remark on the last feature. Our method can be already used to investigate dependencies of a neural network as done in Masud and Borisyuk (2011), i.e. considering pairs of spike trains and performing the aforementioned analysis on each pair. However, it would be interesting to investigate also the existence of triplets, quartets, etc. of dependencies. Using the copula method, this would request the investigation of k dimensional copulas, for $k>2$, and the results may present difficulties of illustration, due to the impossibility to use scatterplots. Using the Cox method, this study would become even more difficult, since one should redefine the hazard function φ in a proper way, e.g. switching from φ_A to a function for the k involved neurons.

Two drawbacks of the Copula method are that sometimes this method does not catch small dependencies and it requests a large sample size to estimate the Kendall's tau properly.

The main advantages of the Cox method are that:

- it is reliable also for small sample size (i.e. 50 data for each train);
- it allows to ignore the “spurious”connection, distinguishing between direct and indirect connections and dealing correctly with connectivity due to common source
- it has been already tested in a network of 20 neurons, with satisfactory results.

The main drawback is its dependence on the goodness of the influence function Z_B for the considered data. Furthermore, even choosing a good influence function, the estimation of its parameter, such as τ_s, τ_r for the alpha function, may represent a hard task.

Finally, both methods allow to detect the presence of a delay in the coupling.

Cox and Lewis (1972) underline the complementary role of the study of the occurrence rate of events (as done in the Cox method), and of the ISIs (as done in the copula method) for the theoretical study of point processes. This fact agrees with our results for the statistical study of dependencies between point processes. Hence, a reliable analysis should consider both methods.

6. Conclusions

We have proposed the use of the copula notion to analyze dependencies between two spike trains. This has allowed the development of a new non-parametric method based on the study of their scatterplots and densities, as well as association indexes, such as the Kendall's tau. This method allows to enlighten the effect of an interspike on the subsequent ones of the other neuron. This can be studied checking copula scatterplots and performing a test $H_0: \tau=0$. Furthermore, the use of copulas helps to recognize the direction scheme of two neurons, exchanging the role of target and reference neurons. Finally, considering all this information, one might conjecture the nature of the phenomenon at the origin of the dependencies.

The proposed method can be also applied to experimental data, allowing to catch dependencies. However, it may happen to obtain copula scatterplots with shapes different from those discussed here. To interpret them, it is advisable to enlarge the set of examples, to include cases involving inhibition phenomena or spurious connections. The development of a specific software enclosing copulas and the previously mentioned methods, particularly Cox with a proper influence function Z_B, represents an important step toward a better comprehension of the structure of a network. Our future work will consider the possibility to fit data with suitable copula families.

Finally, a further step will be to consider k-dimensional copulas to investigate the dependencies in groups of k neurons, non pairwise.

Acknowledgments

The authors are grateful to Mohammad Masud and Roman Borisyuk for providing us their codes and softwares, and for some useful suggestions. We also thank Susanne Ditlevsen for her useful comments. This work was partly supported by MIUR, PRIN 2008 and by the University of Turin, local grant.

REFERENCES

Borisyuk, R., 2004. Oscillatory activity in the neural networks of spiking elements. Biosystems 52, 301–306.

Borisyuk, G.N., Borisyuk, R.M., Kirillov, A.B., Kovalenko, E.I., 1985. A new statistical method for identifying interconnections between neuronal network elements. Biol. Cybern. 52, 301–306.

Brillinger, D.R., 1988. Maximum likelihood analysis of spike trains of interacting nerve cells. Biol. Cybern. 59, 189–200.
Capocelli, R.M., Ricciardi, L.M., 1971. Diffusion approximation and first passage time problem for a model neuron. Kybernetik 8, 214–223.
Cox, D.R., 1972. The statistical analysis of dependencies in point processes. In: Lewis, P.A. (Ed.), Stochastic Point Processes, pp. 55–66. New York.
Cox, D.R., Lewis, P.A.W., 1972. Multivariate point processes. Proceedings Sixth Berkeley Symposium on Probability and Mathematical Statistics, 3, pp. 401–448.
Deco, G., Schürmann, B., 1998. Stochastic resonance in the mutual information between input and output spike trains of noisy central neurons. Physica D. 117, 276–282.
Eldawlatly, S., Jin, R., Oweiss, K.G., 2009. Identifying functional connectivity in large-scale neural ensemble recordings: a multiscale data mining approach. Neural Comput. 21, 450–477.
Genest, C., Favre, A.C., 2007. Everything you always wanted to know about copula modeling but were afraid to ask. J. Hydrol. Eng. 12, 347–368.
Genest, C., Rémillard, B., Beaudoin, D., 2009. Goodness-of-fit tests for copulas: a review and a power study. Insurance: Math. Econ. 44 (2), 199–213.
Gerstner, W., Kistler, W.M., 2002. Spiking Neuron Models: Single Neurons, Populations, Plasticity. Cambridge University Press.
Grün, S., Rotter, S., 2010. Analysis of parallel spike trains, In: Grun, S., Rotter, S. (Eds.), 1st ed. Springer.
Jenison, R.L., Reale, R.A., 2004. The shape of neural dependence. Neural Comput. 16 (4), 665–672.
Lansky, P., 1984. On approximations of Stein's neuronal model. J. Theoret. Biol. 107, 631–647.
Masud, M.S., Borisyuk, R., 2011. Statistical technique for analyzing functional connectivity of multiple spike trains. J. Neurosci. Methods 196 (1), 201–219.
Musila, M., Lansky, P., 1991. Generalized Stein's model for anatomically complex neurons. Biosystems 25, 179–191.
Nelsen, R.B., 2006. An Introduction to Copulas. Springer, United States of America.
Onken, A., Grünewälder, S., Munk, M.H.J., Obermayer, K., 2009. Analyzing short-term noise dependencies of spike-counts in macaque prefrontal cortex using copulas and flashlight transformation. PLoS Comput. Biol. 5, e1000577.
Perkel, D.H., Gerstein, G.L., Moore, G.P., 1967. Neuronal spike trains and stochastic point processes II. Simultaneous spike trains. Biophys. J. 7, 419–440.
Sacerdote, L., Sirovich, R., 2010. A copulas approach to neuronal networks models. J. Physiol. Paris 104, 223–230.
Sacerdote, L., Tamborrino, M., 2010. Leaky Integrate and Fire models coupled through copulas: association properties of the Interspike Intervals. Chin. J. Physiol. 53 (6), 396–406.
Sirovich, L., 2003. Dynamics of neuronal populations: eigen function theory; some solvable cases. Comput. Neural Syst. 14, 249–272.
Sirovich, R., 2006. Mathematical models for the study of synchronization phenomena in neuronal networks. Ph.D. Thesis.
Sirovich, R., Sacerdote, L., Villa, A.E.P., 2007. Effect of increasing inhibitory inputs on information processing within a small network of spiking neurons. Lect. Notes Comput. Sci. 4507, 23–30.
Stein, R.B., 1965. A theoretical analysis of neuronal variability. Biophys. J. 5, 173–194.
Stevenson, I.H., Rebesco, J.M., Hatsopoulos, N.G., Haga, Z., Miller, L.E., Kording, K.P., 2009. Bayesian inference of functional connectivity and network structure from spikes. Brain Connectivity 17 (3), 203–213.
Tamborrino, M., Sacerdote, L. and Jacobsen, M., submitted for publication. Diffusion approximation and first passage time for multivariate jump processes.
Tetzlaff, T., Rotter, S., Stark, E., Abeles, M., Aertsen, A., Diesmann, M., 2008. Dependence of neuronal correlations on filter characteristics and marginal spike train statistics. Neural Comput. 20, 9.
Tuckwell, H.C., Richter, W., 1978. Neuronal interspike time distributions and the estimation of neurophysiological and neuroanatomical parameters. J. Theor. Biol. 71, 167–183.